Journal of Asian Earth Sciences 46 (2012) 161–176

Contents lists available at SciVerse ScienceDirect

Journal of Asian Earth Sciences

journal homepage: www.elsevier.com/locate/jseaes

Receiver function structure beneath four seismic stations in the Sumatra region

Kenneth A. Macpherson [a,*], Dannie Hidayat [a], Siang Huat Goh [a,b]

[a] Earth Observatory of Singapore, Nanyang Technological University, Singapore
[b] Department of Civil Engineering, National University of Singapore, Singapore

ARTICLE INFO

Article history:
Received 20 May 2011
Received in revised form 10 November 2011
Accepted 1 December 2011
Available online 6 January 2012

Keywords:
Receiver functions
Crustal thickness
Sumatra
Teleseismic

ABSTRACT

We estimated the velocity structure beneath four three-component broad-band seismic stations in the Sumatra region by the joint inversion of teleseismic receiver functions and surface wave group velocities. The stations, part of GEOFON network GE, are located in diverse geologic settings including backarc basins, forearc basins, and the forearc ridge. The stations are distributed roughly trench-parallel, providing samples of conditions along the length of Sumatra. 143 receiver functions were computed by employing an iterative, time-domain deconvolution in order to minimize acausal noise. The teleseismic observations at each station were grouped by back azimuth and ray parameter and then stacked to increase the signal to noise ratios. Surface wave group velocity dispersion was measured for paths across the Sunda block from events to the northeast of the stations. *P*-wave velocity profiles were derived by inverting the stacks and group velocity data using a linearized time-domain inversion scheme with an interpolated CRUST2.0 global model for input. The results differ significantly from CRUST2.0, and reflect the diversity of geologic environments within which the stations are located. Crustal thicknesses beneath the stations range from 16.0 km at the forearc to 30.0 km at a backarc basin. These results add to the available velocity and crustal thickness data for the Sumatra region.

1. Introduction

The Sumatra region, one of the most seismically active zones on earth, has produced three great earthquakes ($M_w \geqslant 8.5$) since the 2004 Boxing day earthquake (Lange et al., 2010). In addition to the tsunami hazard posed by these large subduction zone events, the long-period strong ground motions they induce threaten population centers as far from the margin as Singapore (Megawati and Pan, 2009; Pan and Sun, 1996). Further, on Sumatra and its environs, there is significant population and infrastructure exposed to the seismic hazard. The Indonesian city of Padang, with a population of approximately 850,000, was severely damaged by the September 30, 2009 $M_w = 7.6$ earthquake, and is situated near a portion of the margin that has not ruptured since 1797 (McCloskey et al., 2010), and where super-cycle patterns indicate a $M_w \approx 8.8$ event could occur in the coming decades (Sieh et al., 2008).

Many of the techniques for quantifying seismic hazards, such as ground-motion simulations and earthquake locations, require realistic earth models as input (Magistrale et al., 2000). For the Sumatra region, velocity data is available in the form of low-resolution global data sets such as CRUST2.0 Bassin et al. (2000), high-resolution reflection profiles, e.g. (Franke et al., 2008), and the previously published receiver function study of Kieling et al. (2011). However, because these data sets are either located at isolated sampling locations or are of a low resolution, additional data are needed in order to build a velocity model of sufficient resolution to be useful for hazard studies. As a way to add to the database of available velocity information for the Sumatra region, we investigated the receiver function structure beneath four broad-band seismic stations.

1.1. Geologic and seismotectonic setting

The island of Sumatra lies along the southwestern boundary of the Sundaland craton, forming an Andean continental margin (see Fig. 1) (Milsom, 2005). The geology of the region is characterized by forearc and backarc basins associated with the subduction front. These basins are filled primarily with sedimentary and volcanic material of Tertiary age (Barber et al., 2005). Pre-Tertiary basement crops-out in the Barisan mountains where it is often overlain by recent volcanic deposits.

The seismotectonics of the Sumatra region are dominated by the Sunda megathrust, a subduction front formed by the convergence of the Indo-Australian plate and the overriding Eurasian plate (see Fig. 1). Ongoing subduction is indicated by active volcanism in the Barisan mountains along the west coast of the island as well as the presence of a Wadati-Benioff zone (Milsom, 2005). Convergence vectors vary considerably along the Sumatran portion of the Sunda arc due to the east African location of the pole of rotation

* Corresponding author. Tel.: +65 9383 9509; fax: +65 6790 1585.
E-mail address: kamacpherson@ntu.edu.sg (K.A. Macpherson).

1367-9120/$ - see front matter © 2011 Elsevier Ltd. All rights reserved.
doi:10.1016/j.jseaes.2011.12.005

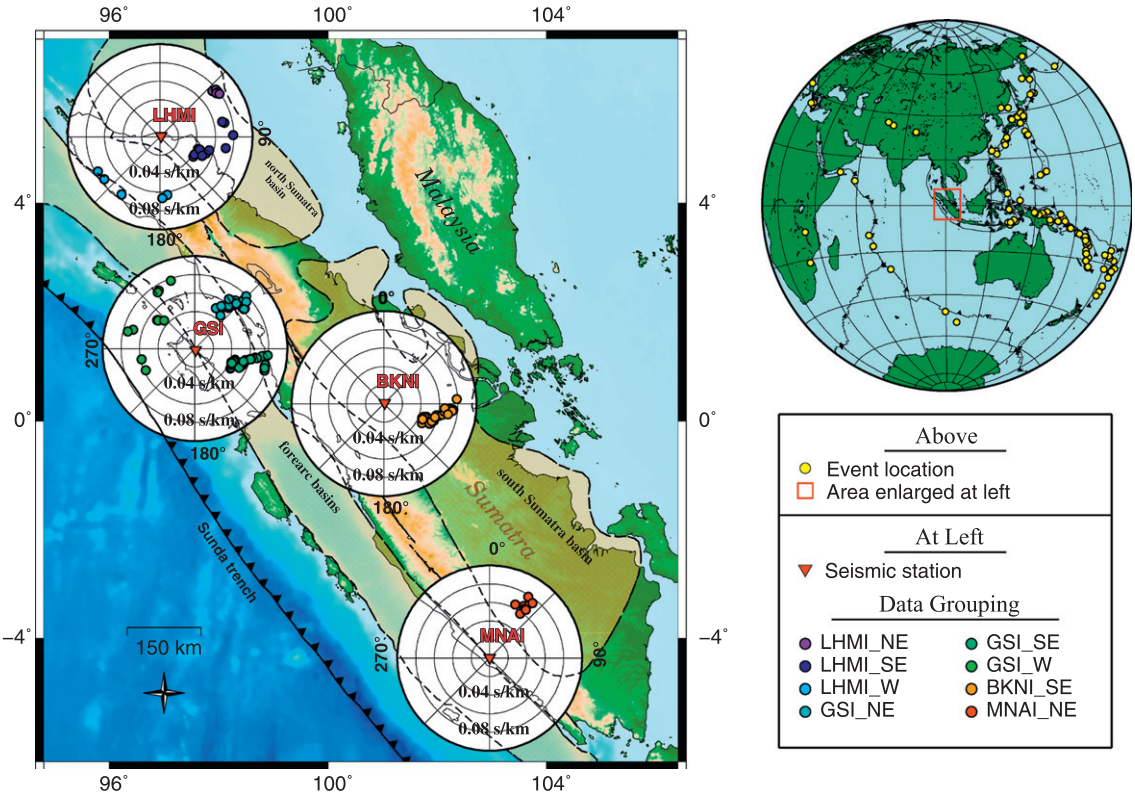

Fig. 1. Study area showing the locations of the four seismic stations in the Sumatra region. The globe shows the locations of the teleseismic events that were used to compute receiver functions. The polar plots around each station show the observations plotted in back azimuth-ray parameter space. The data groupings that were used to stack observations are color coded. The areal extent of the major basins in the region are also shown (basin boundaries are from Working Group on Resource Assessment (1991)).

as indicated by geographic positioning system data (Larson et al., 1997). Rates of convergence range from approximately 60 millimeters per year (mm/yr) in the south to 50 mm/yr in the north, with the convergence becoming increasingly oblique from south to north. The strike-slip component of motion induced by this oblique convergence is accommodated by the great Sumatran fault, a right-lateral fault running the length of Sumatra along the spine of the Barisan mountains (Sieh and Natawidjaja, 2000). The complex Sumatran platelet, or sliver, between the trench and the great Sumatran fault contains the forearc basins and forearc ridge, and is considerably deformed. Another trench-parallel right-lateral fault system, the Mentawai fault, whose trace runs along the outer edge of the forearc basins, accommodates additional strike-slip motion and may delineate the boundary between the accretionary complex and continental backstop (Diament et al., 1992).

2. Receiver functions

The inversion of teleseismic receiver functions is a strategy that is commonly employed to determine the velocity structure beneath three-component seismic stations, e.g., Langston (1977), Ammon and Zandt (1993), Searcy et al. (1996), Midzi and Ottemoller (2001), Park et al. (2009), Wang et al. (2010). The receiver function technique exploits the fact that *P*-to-*S* converted waves have higher amplitudes in the radial component than in the vertical. By deconvolving the vertical from the radial components of three-component recordings, a time-series that is primarily a function of converted waves is produced:

$$H(\omega) = \frac{S(\omega)R(\omega)}{S(\omega)V(\omega)} = \frac{R(\omega)}{Z(\omega)} \quad (1)$$

where R and V are the radial and vertical components, respectively, S is the source spectrum, and ω is the radial frequency (Ammon, 1991). Note that the deconvolution has the added benefit of removing the source factor from the receiver function. Under the assumptions that the sampled geological interfaces are flat and that waves are steeply incident, receiver functions retain many of the properties of seismograms, with arrivals representing the response of the radial component to the incident plane wave. The *P*-to-*S* converted wave arrivals in the receiver function can be modeled to provide constraints on the Moho depth and the crustal velocity structure. Frequency content is controlled via a Gaussian filter of the form:

$$G(\omega) = \exp\left(\frac{-\omega^2}{2a^2}\right) \quad (2)$$

where a is a factor that controls the width of the filter.

2.1. Deconvolution

Because of the low signal to noise ratios of the majority of the data considered in this study, receiver functions were computed using the time-domain iterative deconvolution technique of Ligorria and Ammon (1999) rather than a more conventional frequency domain deconvolution. The iterative deconvolution derives receiver functions by minimizing the difference between the observed radial component and the convolution of the observed vertical component and a spike train that is updated iteratively. It has been shown that this technique, while slightly less efficient than frequency domain deconvolutions, produces comparable results with low-noise data, and can considerably reduce acausal noise in less ideal data due to the flat spectral response at long periods of the time-domain signals (Ligorria and Ammon, 1999). Fig. 2 shows a comparison of receiver functions computed by the iterative and frequency domain schemes. Both traces have a Gaussian filter applied with a width of 1.5, which filters frequencies above approximately 0.75 Hz. Note